



HAL
open science

Determination of 3D fiber orientations in reinforced thermoplastics, using scanning electron microscopy

Luc L. Averous, Jean-christophe Quantin, Dominique Lafon-Pham, Alain Crespy

► **To cite this version:**

Luc L. Averous, Jean-christophe Quantin, Dominique Lafon-Pham, Alain Crespy. Determination of 3D fiber orientations in reinforced thermoplastics, using scanning electron microscopy. *Acta Stereologica*, 1995, 14 (1), pp.69-74. hal-02927869

HAL Id: hal-02927869

<https://imt-mines-ales.hal.science/hal-02927869>

Submitted on 31 Aug 2021

HAL is a multi-disciplinary open access archive for the deposit and dissemination of scientific research documents, whether they are published or not. The documents may come from teaching and research institutions in France or abroad, or from public or private research centers.

L'archive ouverte pluridisciplinaire **HAL**, est destinée au dépôt et à la diffusion de documents scientifiques de niveau recherche, publiés ou non, émanant des établissements d'enseignement et de recherche français ou étrangers, des laboratoires publics ou privés.

DETERMINATION OF 3D FIBER ORIENTATIONS IN REINFORCED THERMOPLASTICS,
USING SCANNING ELECTRON MICROSCOPY

Luc Avérous, Jean C. Quantin, Dominique Lafon, Alain Crespy

Ecole des Mines d'Alès, Laboratoire matrices-matériaux minéraux et
organiques, 6 avenue de clavières, 30319 Alès, France

ABSTRACT

This paper describes techniques allowing the determination of three-dimensional orientations of fillers, in fiberglass reinforced thermoplastics, using scanning electron microscopy. To measure orientation angles (in-plane and inclination angles), it's necessary to individualize each particle. Segmentation operations are done by watershed on a filtered distance function. Two sectioned surfaces with different section angles must be studied, to construct the total 3D orientation distributions. A good representation of results is given by density stereographic projection, that offers very synthetic informations.

Key words: fiberglass reinforced thermoplastics, scanning electron microscopy, segmentation, three-dimensional orientation distributions.

INTRODUCTION

Fiberglass reinforced thermoplastics are increasingly used in a great number of applications. Fibers bring to the thermoplastic matrix, better mechanical properties like stiffness, impact resistance, etc... Properties of such materials depend strongly on microtextural characteristics (Guild and Summerscales, 1993; Avérous et al., 1994) such as fiber orientations. So, using image analysis, we investigate fibers orientation distributions, in order later to establish correlations with macroscopic properties.

When material is sectioned and the surface polished, the elliptical mark of the fiber is used to determine the orientation Euler angles (ϕ in-plane angle and θ inclination angle) (see Fig. 2).

In the last decade, some authors have followed similar approaches. Using reflection microscopy: Fischer and Eyerer (1988), Toll and Andersson (1991), O'Connell and Duckett (1991), Hine et al. (1993) developed processes of orientation determinations. But, for the same ellipse we get two possible orientation angles. And, these approaches do not manage totally the problem of ambiguity of 180° on ϕ determination.

To the authors' knowledge, only Archenhold, Clarke and Davidson (1992; 1993), using a confocal scanning laser microscope, propose a process allowing to determine real three-dimensional orientations. Unfortunately, this type of instrument is until now, expensive and not very usual.

We propose, using a scanning electron microscopy (S.E.M.), to get the same kind of characterizations.

MATERIALS AND METHODS

In this study, the thermoplastic used is polypropylene, containing 30% by weight of short fiberglass. Cut thread provides fibers whose length is typically 100 microns and the diameter 13 microns.

The material is supplied in the form of end-gate injection bar (section: $10 \times 4 \text{ mm}^2$)

Once the bar sectioned, great care must be taken to the preparation of the surface by polishing with finer and finer abrasive.

The full section under study is sampled in investigation zones of equal surface ($1 \times 1 \text{ mm}^2$), using a diamond point.

Observations are done by electronic microscopy (backscattered electrons) with a high accelerating voltage in order to get an important focus depth. So, it is possible to detect the plunge sense of the fiber, the direction of penetration; using as indicator, the clearer trail visible at an extremity of the ellipse (see Fig. 4 and 5).

The image analysis system is composed by a personal computer (Intel i486), a digitalization card (Matrox 1024) and a dedicated image analysis software (Visilog version 3.6).

Images are transferred from the S.E.M. (Jeol 35CF) to the image analysis system directly through electronic connections. Electronic deformations are corrected by interpolation transformations on images. We obtain grey level images of 512×340 pixels (see Fig. 4).

Treatment of grey level images is quite simple. Top hat transformations (Serra, 1982; Coster et al., 1989) are processed to clean the picture. After thresholding operations, it is necessary to separate touching fibers, in order to individualize and labelize each one.

For the separation of connected particles, we use as marker the proximity of two reflex angles. Segmentations are done in several phases. First, the binary image must be filtered, we eliminate artefacts and fibers' ends by operations of erosion/reconstruction. Then, we process a distance function on the cleaned image.

But a determination of watershed lines (Beucher, 1990) on the inverted distance function leads to oversegmentation. The particle could be cut into two connected elements by a simple noise on the particle contour (Gratin et al., 1991).

So at first, it is necessary to filter the distance function. Our approach is to subtract maximas functions to the initial distance function (see Fig. 1).

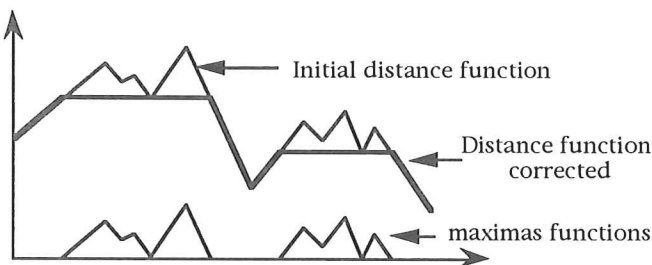


Fig. 1. Filtering of distance function.

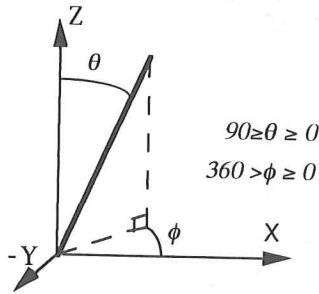


Fig. 2. Definition of axes and angles.

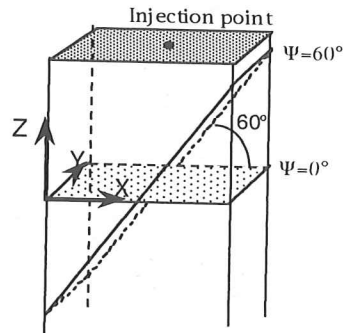


Fig. 3. Definition of section angle.

Once touching fibers separated (see Fig. 6), we can measure on each particle parameters to determine later inclination angles.

The in-plane angle ϕ is calculated using second moments of inertia (Stobie, 1986):

$$\phi = \frac{1}{2} \tan^{-1} [2M_{12} / (M_{20} - M_{02})]$$

The in-plane angle ϕ presents a first indetermination of 90° , removed using the sign of difference between M_{20} and M_{02} .

To remove the ambiguity of 180° that remains on ϕ , we use the shift of the particle centroids between two binary images (see Fig. 5), result of a double threshold (low and higher) on a same cleaned grey level image. Between the first and second thresholded image, we note an evolution of the particles centroids from which, we can determine plunge sense of fibers. The centroids are measured by determination of the first moments M_{10} and M_{01} on each labeled particle.

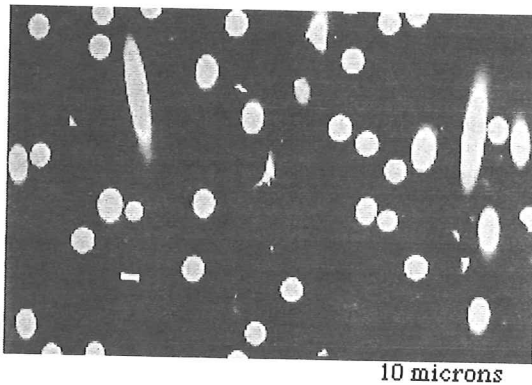


Fig. 4. Grey level image.

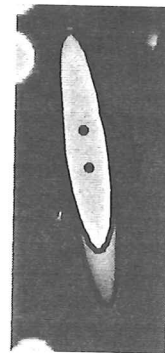


Fig. 5. Shift of centroids with threshold levels.

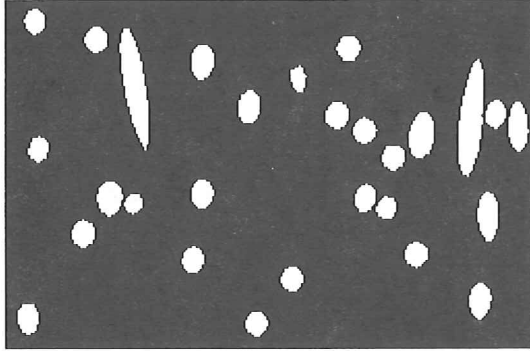


Fig. 6. Binary image filtered with separated particles.

Generally, the inclination angle θ is determined by: $\theta = \cos^{-1}(a/b)$. Parameter "a" is the minor axis length and "b" the major axis length of the particle. But, the factor "a" could be advantageously substituted (Toll et al., 1991) by $4 \cdot \text{area} / (\pi \cdot b)$.

Stobie (1980) determined parameters a et b, using the second moments. This approach, we have tested, seems to be less sensible to noises on the particle contours. So, we calculate θ by the equations:

$$a^2 = 2(M_{20} + M_{02}) + 2[(M_{20} - M_{02})^2 + 4M_{11}^2]^{\frac{1}{2}}$$

$$b^2 = 2(M_{20} - M_{02}) - 2[(M_{20} - M_{02})^2 + 4M_{11}^2]^{\frac{1}{2}}$$

The probability for a fiber to be cut, and to be entirely included in the measure mask (fibers adjacent to the measure mask are eliminated) is a function of the inclination angle. So, to remove this bias, each selected fiber is weighted by $1/|\cos \theta|$ (Stoyan et al., 1987).

For a nearly circular particle, $\theta < 30^\circ$ (Clarke et al., 1991), error involved in the determination of the inclination angle is important and produces a strong incertitude zone. An approach is to cut the sample at a different angle, $\Psi=60^\circ$, from the precedent sectioned surface (see Fig. 3), producing a different incertitude zone.

For $\Psi > 0$, using Euler angles, it's necessary to convert apparent angles ($\theta(\Psi=60), \phi(\Psi=60)$) to ($\theta(\Psi=0), \phi(\Psi=0)$) (Archenhold et al., 1992).

With both populations, it is possible to reconstruct all the orientation distributions without particular incertitude zone.

Advantageously, synthetic results of orientation distributions are presented on stereographic projection. Fibers are projected on inferior hemisphere.

RESULTS-DISCUSSIONS.

The sampling strategy adopted during this study is relative to the injection process. So, using the two planes of symmetry, we investigate only a quarter of the studied section (see Fig. 7).

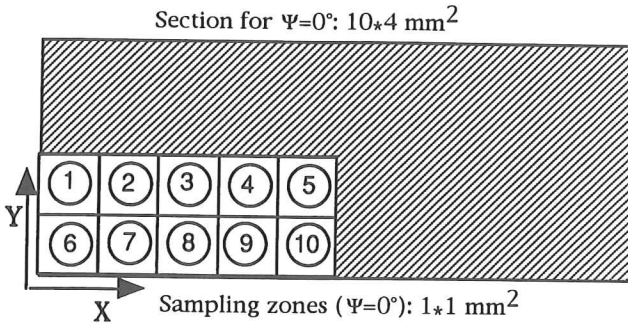


Fig. 7. Sampling strategy for a section perpendicular of injection direction.

We determine 10 sampling zones of equal area; each one, is described by image frames. Hundreds of fibers are analyzed for each zone.

Results presented in Fig. 8 are very significant. We present for each determined sampling zone the stereographic plot of density.

Principal fibers orientations are marked by highest densities. We can note a different orientational state between the skin (border) and the heart (center) of the end-gate injection bar.

In this case, with this polymer and these fibers, with these conditions of process: fibers nearest the border are parallel to the border. On the other hand, fibers orientation is less notable in core.

Perspectives of this study are important and notably establish relationship between fibers orientation and thermo-mechanical properties of the material.

Except, this orientational point, microtextural characteristics are also described by other aspects such as the dispersion of fibers in the matrix.

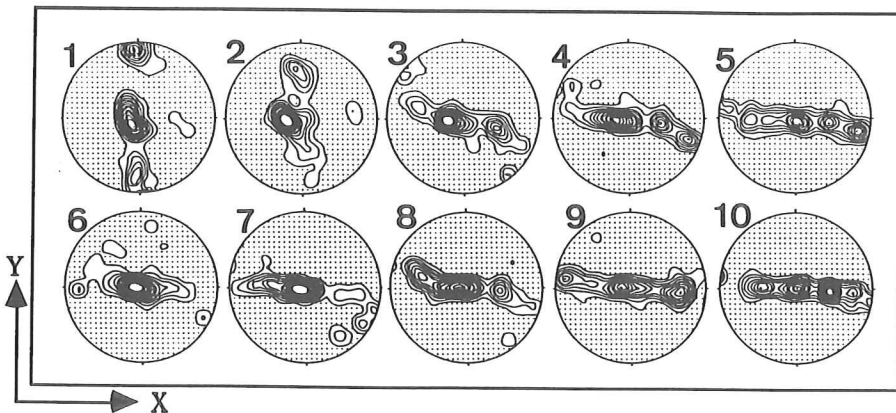


Fig. 8. Density stereographic plots.

REFERENCES

- Archenhold G, Clarke A, Davidson N. 3D microstructure of fibre reinforced composites. SPIE Biomedical Image Processing and Three-Dimensional Microscopy 1992; 1660: 199-210.
- Avérous L, Quantin JC, Lafon D, Crespy A. Microtextural characterization of fiberglass reinforced polypropylene : Effect of the filler size. Les Diablerets, Switzerland: ISPAC-7, 1994.
- Beucher S. Segmentation d'images et Morphologie mathématique. Thèse de L'Ecole Nationale Supérieure des Mines de Paris, 1990.
- Clarke A, Davidson N, Archenhold G. A large area, high resolution image analyser for polymer research. Sunnyvale CA: Transputing'91, 1991: 31-47.
- Clarke A, Davidson N, Archenhold G. Measurements of fibre direction in reinforced polymer composites. J Micros 1993; 171: 69-79.
- Coster M, Chermant JL. Précis d'analyse d'images. Presses du CNRS, 1989.
- Fischer G, Eyerer P. Measuring spatial orientation of short fiber reinforced thermoplastics by image analysis. Polymer Composites 1988; 9: 297-304.
- Gratin C, Meyer F. Mathematical morphology in three dimensions. Acta Stereol 1991; 11: 551-558.
- Guild FJ, Summerscales J. Microstructural image analysis applied to fibre composite materials : a review. Composites 1993; 24: 383-393.
- Hine PJ, Duckett RA, Davidson N, Clarke AR. Modelling of the elastic properties of fibre reinforced composites I : Orientation measurement. Composites Science and Technology 1993; 47: 65-73.
- O'Connell PA, Duckett RA. Measurements of fibre orientation in short-fibre-reinforced thermoplastics. Composites Science and Technology 1991; 42: 329-347.
- Serra J. Images analysis and mathematical morphology. New York: Academic Press, 1982.
- Stobie RS. Analysis of astronomical images using moments. Journal of the British Interplanetary Society 1980; 33: 323-326.
- Stoyan D, Kendall WG, Mecke J. Stochastics geometry and its applications. Chichester: J Wiley & Sons, 1987.
- Toll S, Andersson PO. Microstructural characterization of injection moulded composites using images analysis. Composites 1991; 22: 298-306.